

## Strong anisotropies in MBE-grown Co/Cr(001): Ferromagnetic-resonance and magneto-optical Kerr-effect studies

F. Schreiber

*Institut für Experimentalphysik, Ruhr-Universität Bochum, 44780 Bochum, Germany*

Z. Frait

*Institute of Physics, Czech Academy of Sciences, 18040 Prague, Czech Republic*

Th. Zeidler, N. Metoki,\* W. Donner,† H. Zabel, and J. Pelzl

*Institut für Experimentalphysik, Ruhr-Universität Bochum, 44780 Bochum, Germany*

(Received 12 August 1994)

Ferromagnetic-resonance (FMR) and magneto-optical Kerr-effect (MOKE) studies of molecular-beam-epitaxy grown Co/Cr(001) superlattices and single layers are presented. The FMR measurements were performed in different sample orientations and in a broad frequency range (9–92 GHz). MOKE hysteresis loops were detected in polar and in longitudinal configuration. The in-plane anisotropy parameters,  $K_1$  and  $K_2$ , the out-of-plane anisotropy (i.e., the effective magnetization including the surface anisotropy,  $K_s$ ), and the  $g$  factor were determined for these samples, which exhibit an anomalous out-of-plane lattice expansion of the hcp Co(11 $\bar{2}$ 0) on bcc Cr(001) as a precursor of a structural phase transition. Due to the strong in-plane anisotropy the switching of the magnetization to out-of-plane easy axis can occur at lower thicknesses ( $\approx 14$  Å) than the change of sign of the effective magnetization ( $\approx 21$  Å). In the intermediate thickness range a peculiar situation can be found with the orientation of the magnetization along the surface normal lying energetically *between* the in-plane easy and hard axis. Taking into account these effects as well as a reduced magnetic moment,  $K_s \approx 0.76$  erg/cm<sup>2</sup> is found. For thin Co layers the  $g$  factor is found to be increased in comparison with the bulk value. This indicates modifications of the electronic properties accompanied with the considerable structural changes.

### I. INTRODUCTION

The investigation of epitaxial thin films is currently one of the major fields in magnetism. Among the properties of these systems, the magnetic anisotropy (in the film plane as well as out-of-plane) and coupling effects belong to the most exciting and most intensively investigated ones.<sup>1,2</sup> The epitaxial growth cannot only be exploited to obtain the desired atomically flat interfaces in order to study magnetism in reduced dimensions but also to stabilize metastable crystallographic phases which cannot be prepared as bulk samples.<sup>3</sup> A particularly interesting example for this is the epitaxial stabilization of bcc Co on GaAs,<sup>3–5</sup> yielding a lattice constant ( $\approx 2.8$  Å) which could be shown to correspond to a metastable state of Co also in theoretical calculations.<sup>6</sup> With the help of these metastable phases very fundamental questions of the relationship between structural and magnetic properties can be investigated.

Co is a good subject for studies of the connection between structure and magnetism. At room temperature the bulk phase of Co is hcp. In the form of thin films Co can also be prepared in two other important structures of the transition-metal series, namely fcc,<sup>7,8</sup> and bcc,<sup>4,5,9</sup> both in different orientations.

In the present study, we are dealing with Co grown epitaxially on bcc Cr(001). Cr has a bulk lattice constant of 2.885 Å which is close to that of bcc Co. It should there-

fore induce significant structural changes of the Co in comparison to the pure hcp structure, accompanied by effects on the magnetic properties as well. We have recently reported the successful growth of epitaxial Co/Cr(001) superlattices and explained the specific problems of the sample preparation and structure of this system.<sup>10,11</sup> Some indications of the rather remarkable properties of the heavily distorted structure of Co on Cr(001) such as perpendicular anisotropy have already been reported in a previous publication.<sup>12</sup> We note that *epitaxial* Co on Cr should not be confused with the alloy system Co-Cr which is very important from the point of view of magnetic anisotropy and its applications.<sup>13</sup> The relevant mechanisms in the latter system are completely different from those in our samples.

In this paper, we present a detailed and comprehensive ferromagnetic-resonance (FMR) and magneto-optical Kerr effect (MOKE) study of Co/Cr(001). We demonstrate the evaluation of the out-of-plane anisotropy in the presence of a strong in-plane anisotropy resulting in significantly different critical thicknesses for the change of sign of the effective out-of-plane anisotropy and for the switching of the equilibrium position of the magnetic moment. In addition, we provide an analysis of the  $g$  factor which can be an important indicator of changes of microscopic origin.

The paper is organized as follows. In Sec. II, we present some basic results of the sample preparation and

characterization as well as the experimental techniques. The energy relations and resonance conditions will be explained in Sec. III. Section IV is devoted to the measurements and their analysis. We will first show some typical results and then discuss the anisotropy parameters and the  $g$  factor. A summary is given in Sec. V.

## II. SAMPLE PREPARATION AND EXPERIMENTAL

The sample preparation was carried out in a commercial metal molecular-beam-epitaxy (MBE) system (Riber EVA32) with a base pressure of  $\sim 4 \times 10^{-9}$  Pa and a working pressure better than  $\sim 6 \times 10^{-9}$  Pa. The growth of the samples was observed *in situ* by reflection high-energy electron diffraction (RHEED). We have used  $\text{Al}_2\text{O}_3$  (1 $\bar{1}$ 02) substrates with a Nb(001) buffer layer onto which an additional Cr(001) layer of about 500 Å thickness was grown. This was followed by the evaporation of the first Co layer.

The samples under investigation are single layers and superlattices, the latter designated as  $[\text{Co}_x\text{Cr}_y]_N$ .  $x$  and  $y$  denote the Co and Cr thickness in Å, respectively, and  $N$  is the number of periods. All samples were thoroughly characterized by means of x-ray-scattering techniques in various configurations such as high-angle, low-angle, and grazing incidence geometry.<sup>10,11</sup> Additional diffuse scattering studies are in progress.<sup>14</sup>

Here we only give a short summary of the structural properties. We find that Co grows on bcc Cr(001) in the hcp phase in the (11 $\bar{2}$ 0) orientation with its  $c$  axis parallel to the [110] axis of Cr. The investigation of the lattice parameters reveals an anomalous out-of-plane expansion of the Co layers, i.e., a structural distortion with a non-Poisson-like elastic behavior which is considered as a precursor of a structural transition from the hcp to the bcc phase.<sup>10,11</sup> The bcc phase of Co is, however, not reached in this epitaxial system even for the samples with the thinnest Co layers.

As the uniaxial (hcp) Co structure is grown on a crystallographic plane with fourfold symmetry there are two equivalent orientations for the  $c$  axis perpendicular to each other. This can give rise to a twinned structure of  $c$  axes which has to be taken into account in the analysis of the magnetic parameters (see Sec. III).

The FMR experiments were performed at 9, 17, 25, 48, 69, and 92 GHz in fields up to 31 kOe. This very broad frequency range is particularly useful if samples with strong in-plane anisotropies are investigated and if the whole series covers a big range of out-of-plane anisotropies, as it is the case here. In addition, measurements at several frequencies enable the determination of the anisotropy parameters and the  $g$  factor with reasonable error bars even if the resonance linewidths are quite large. A standard rectangular TE<sub>102</sub> cavity was used at  $X$  band whereas for the higher frequencies the sample was placed in a shortened waveguide setup. The samples were measured as a function of the in-plane angle and in the out-of-plane configuration. The absolute accuracy of the apparatus for measurements of the microwave frequency and the static magnetic field was better than  $10^{-7}$  and  $10^{-3}$ , respectively. However, the precision of the deter-

mination of the resonance field,  $H_{\text{res}}$ , depends also on the signal-to-noise ratio and the linewidth,  $\Delta H$  (see Sec. IV for remarks on  $\Delta H$ ). For the present samples the accuracy of the  $H_{\text{res}}$  value was typically better than  $10^{-1}$  kOe.

Hysteresis loops were detected using MOKE in the longitudinal (with fields up to 10 kOe) and in the polar configuration (up to 18 kOe). All magnetic investigations reported here were performed at room temperature.

Although usually the sensitivity of FMR as well as of MOKE is sufficient for the detection of single layers we will concentrate mainly on superlattices as they offer the possibility of a more detailed structural characterization by means of x-ray scattering which is extremely important especially for the system Co/Cr(001).

## III. ENERGY RELATIONS AND RESONANCE CONDITIONS

### A. Samples with one crystallographic domain

The magnetocrystalline anisotropy of uniaxial crystals up to second order is expressed, in general, as

$$F_{\text{ani}} = K_1 \sin^2 \alpha + K_2 \sin^4 \alpha \quad (1)$$

with  $\alpha$  as the angle between the magnetization and the  $c$  axis. The detection of higher than second-order terms is difficult but, in some cases, feasible (see, e.g., Refs. 15 and 16). For our measurements on Co/Cr(001) it is fully sufficient to consider  $K_1$  and  $K_2$  only.

We use a coordinate system in which the magnetization  $\mathbf{M}$  makes a polar angle  $\Theta$  with respect to the film normal and an azimuthal angle  $\phi$  in the film plane with respect to the  $c$  axis. The orientation of the external magnetic field  $\mathbf{H}$  is described by the angles  $\Theta_H$  and  $\phi_H$ . In this coordinate system the magnetocrystalline anisotropy energy density from Eq. (1) takes the form

$$F_{\text{ani}}(\Theta, \phi) = K_1 + K_2 - (K_1 + 2K_2) \sin^2 \Theta \cos^2 \phi + K_2 \sin^4 \Theta \cos^4 \phi. \quad (2)$$

The constant terms will be dropped in the following. Furthermore, the magnetically relevant part of the total free-energy density,  $F_{\text{tot}}$ , contains the interaction with the external field ( $-\mathbf{H} \cdot \mathbf{M}$ ), the demagnetizing (shape anisotropy) energy ( $-2\pi M^2 \sin^2 \Theta$ ), and the surface anisotropy contribution. The latter is usually taken into account by the term  $(2K_s/t_{\text{Co}}) \sin^2 \Theta$  resulting in the effective magnetization

$$4\pi M_{\text{eff}} = 4\pi M - 2 \frac{2K_s}{Mt_{\text{Co}}}. \quad (3)$$

The resonance condition for measurements with the external field  $H$  in the film plane using the above form of the anisotropy energy then reads<sup>17</sup>

$$\left[ \frac{\omega}{\gamma} \right]_{\parallel}^2 = [H \cos(\phi - \phi_H) + 4\pi M_{\text{eff}} + (2H_{A1} + 4H_{A2}) \cos^2 \phi - 4H_{A2} \cos^4 \phi] \times [H \cos(\phi - \phi_H) + (2H_{A1} + 2H_{A2}) \cos(2\phi) - 2H_{A2} \cos(4\phi)] \quad (4)$$

according to standard theory of FMR.<sup>18,19</sup>  $\gamma = g\mu_B/\hbar$  is the gyromagnetic ratio,  $g$  the  $g$  factor, and  $H_{Ai} = K_i/M$ . For the out-of-plane configuration, i.e.,  $\Theta = \Theta_H = 0$ , the resonance condition is

$$\left[ \frac{\omega}{\gamma} \right]_{\perp}^2 = [H - 4\pi M_{\text{eff}} - (2H_{A1} + 4H_{A2})] \times [H - 4\pi M_{\text{eff}}]. \quad (5)$$

### B. Samples with two crystallographic domains

The above relations hold for the case of samples with *only one*  $c$  axis, i.e., only one crystallographic domain. As it was already explained in Sec. II, for Co with  $(11\bar{2}0)$  orientation on a Cr(001) plane with its fourfold symmetry, there may exist an equivalent second crystallographic domain with its  $c$  axis also in-plane but perpendicular to the first one.

In the presence of a second  $c$  axis one has to distinguish between the case of magnetically coupled crystallographic domains and that of uncoupled domains. Further, the difference between the signal generation of FMR and that of hysteresis measurements has to be taken into account.

If the two domains are uncoupled the anisotropy energy has the same form as in Eq. (2) for *each domain* with only the angle  $\phi$  shifted by  $90^\circ$  for the second domain, because the reference direction for the magnetization is the  $c$  axis of the particular domain.

In the FMR experiment two lines will be observed with a uniaxial in-plane angular dependence of each line (but easy axes differing by  $90^\circ$ ) and with intensities proportional to the relative fractions of the two domains,  $x_1$  and  $x_2$  (with  $x_1 + x_2 = 1$ ). This possibility of detecting magnetically nonequivalent constituents of a sample by their respective resonances (provided that they are not strongly coupled) is a specific feature of the FMR technique. It was already used, e.g., to separate regions which differ with regard to their *out-of-plane* anisotropy behavior in investigations of Co-Cr alloys.<sup>13</sup>

In contrast, measurements of the hysteresis of a sample yield a superposition of different subsystems in the sense that they lead to *averaged* magnetic parameters. This applies to, e.g., vibrating sample magnetometry (VSM), superconducting quantum interference devices, and also MOKE (as long as the magnetically different parts are illuminated simultaneously by the spot of the probe laser which is essentially the case for our experiment here). Using these integrating and static methods one cannot, in principle, distinguish between the case of uncoupled and that of coupled domains which is described below. If both domains are equivalent and contribute 50% to the signal, an effective fourfold in-plane anisotropy will be observed, and the separation of the anisotropy parameters of different order,  $K_1$  and  $K_2$ , will be difficult.

In the other limiting case, when the two domains are strongly coupled, the anisotropy energy density can be considered to have effectively no spatial dependence and to be one and the same for the whole sample. Assuming that  $K_1$  and  $K_2$  have the same values in both domains we

can write

$$F_{\text{ani}}^{(\text{coupled})}(\Theta, \phi, x_1, x_2) = x_1 F_{\text{ani}}(\Theta, \phi) + x_2 F_{\text{ani}}(\Theta, \phi + 90^\circ). \quad (6)$$

In general, this leads to a superposition of a uniaxial and a fourfold anisotropy contribution. For the special case of  $x_1 = x_2 = 0.5$  we end up with an anisotropy energy of the form

$$F_{\text{ani}}^{(\text{coupled})}(\Theta, \phi, x_1 = x_2 = 0.5) = -\frac{1}{2}(K_1 + 2K_2)\sin^2\Theta + \frac{3}{8}K_2\sin^4\Theta + \frac{1}{8}K_2\sin^4\Theta \cos(4\phi), \quad (7)$$

where the latter two terms are equivalent to the energy expression of a cubic (001) plane taking into account first-order cubic anisotropy constants only. The resonance condition then reads for the in-plane orientation

$$\left[ \frac{\omega}{\gamma} \right]_{\parallel}^2 = \{ H \cos(\phi - \phi_H) + 4\pi M_{\text{eff}}^* - \frac{1}{2}H_{A2}[3 + \cos(4\phi)] \} \times [H \cos(\phi - \phi_H) - 2H_{A2}\cos(4\phi)] \quad (8)$$

and for the out-of-plane configuration

$$\left[ \frac{\omega}{\gamma} \right]_{\perp} = H - 4\pi M_{\text{eff}}^* \quad (9)$$

with the modified effective magnetization

$$4\pi M_{\text{eff}}^* = 4\pi M - 2\frac{2K_s}{Mt_{\text{Co}}} + H_{A1} + 2H_{A2}, \quad (10)$$

which comprises all  $\sin^2\Theta$  dependencies of the energy expression.

In the most general case we have to consider two domains which are partly coupled and partly uncoupled. Then we can expect a mixture of the above-mentioned limiting cases, i.e., in the FMR experiment we see two lines with in general different intensities and with in-plane anisotropies which are effectively reduced by the coupled part of the respective other domain. Such a behavior will be analyzed by using the relations of the uniaxial case but then the anisotropy parameters need to be interpreted as *effective* quantities.

## IV. RESULTS AND DISCUSSION

In this section, we first show typical results from samples which exhibit either dominating uniaxial in-plane anisotropy of fourfold symmetry. We present the in-plane angular dependence of the resonance field as well as the out-of-plane line position and compare this with hysteresis loops from MOKE.

The combined investigation by FMR and MOKE is particularly useful in view of the present competition of strong in-plane and out-of-plane anisotropy. With FMR, the determination of the in-plane anisotropy even for samples with a small or negative  $4\pi M_{\text{eff}}$  is possible (as

long as the resonance lines are not too broad). With MOKE, this can be difficult, in contrast to the rather convenient proof of an out-of-plane magnetized sample by the corresponding hysteresis by polar MOKE. Furthermore, FMR and MOKE are complementary in the sense that with MOKE the *hysteresis* is detected whereas with FMR one is usually working in a *saturated* state, and the anisotropy enters via effective torques acting on the magnetization vector when oscillations are excited. The analysis of FMR spectra is therefore independent of assumptions on the magnetization process.

The second part of this section is devoted to the analysis of the results from different samples which are summarized in Table I. The magnetic parameters were determined by fitting simultaneously FMR measurements at different orientations and in the whole broad frequency range and taking into account the MOKE data. Therefore, a reasonable accuracy of the quantities could be achieved in spite of quite broad resonance lines (some hundred Oe to more than 1 kOe).

The exact mechanisms leading to these broad lines are not yet clear, but, of course, for the present heavily strained structure with two crystallographic domains, one cannot expect the lines to be narrow. Furthermore, it had already been remarked in Ref. 20 that there is a general tendency that systems with large anisotropy or magnetostriction exhibit broader resonances. Frequency-dependent measurements of the linewidth revealed that even for a single layer with  $t_{\text{Co}}=60$  Å the main contribution was  $\Delta H(0)$  which is the frequency-independent inhomogeneity parameter.<sup>19</sup> It may be interesting to note that also in metastable bcc Co broad lines were found,<sup>21</sup> significantly broader than those, e.g., in fcc Co.<sup>8</sup>

## A. Measurements

### 1. In-plane uniaxial samples

We concentrate on four superlattices (SL1–SL4) the thicknesses of which exhibit almost equidistant spacing on the  $1/t_{\text{Co}}$  axis. The change of the out-of-plane line position relative to the in-plane line positions and the  $\omega/\gamma$  line (which corresponds to the FMR field for the case of a completely isotropic sample, e.g., a film without in-plane anisotropy and  $4\pi M_{\text{eff}}=0$ , i.e., compensation of demagnetizing and surface anisotropy), gives a good first impression of the trend of the out-of-plane anisotropy to become smaller and, finally, negative with decreasing thickness. In Ref. 22 already from  $H_{\text{in-plane}}^{\text{res}} \rightarrow \omega/\gamma$  for

thin layers the critical thickness of Fe on Ag(001) could be determined. For other examples of the detection of out-of-plane easy axis by FMR in metallic films see, e.g., Refs. 13, 22, and 23. In our case of Co/Cr(001), however, the situation is complicated by a significant in-plane anisotropy, and it can happen that the energetically favorable orientation of the magnetization is still in-plane, in spite of  $H_{\text{perp}}^{\text{res}} < \omega/\gamma$  and  $4\pi M_{\text{eff}} < 0$ . This leads to the definition of two critical thicknesses as explained in the analysis part below.

Superlattice SL 1 ( $t_{\text{Co}}=35$  Å). In Fig. 1(a) we plot the in-plane angular dependence of the resonance field and the out-of-plane line position. In order to allow for a direct comparison of the FMR fields we have chosen an intermediate frequency at which all lines can be observed up to 31 kOe. At higher frequencies it can happen that in perpendicular orientation the line lies at too high fields whereas at very low frequencies the in-plane easy axis resonance may approach zero field. Again, we stress that the lines from all frequencies were considered in the analysis as far as they were accessible. Hysteresis loops with the field along the three principal directions (out-of-plane and in-plane both hard and easy axis) are shown in Fig. 1(b). The strong in-plane anisotropy is obvious. The fact that the perpendicular resonance field is well above the in-plane resonance fields and, equivalently, that the out-of-plane saturation field is higher than that for the in-plane hard axis indicates that the zero-field magnetization is in-plane and that there is a considerable positive  $4\pi M_{\text{eff}}$ . This sample with relatively thick Co layers behaves qualitatively as bulk material. However, *quantitatively* there is a significant difference to bulk parameters already for  $t_{\text{Co}}=35$  Å (in particular the value  $4\pi M_{\text{eff}}=5.7$  kOe is strongly reduced as compared to about 18 kOe of bulk Co).

It should be pointed out that there is an excellent agreement between FMR and MOKE data. For the fit of the FMR data we used the above-mentioned value for  $4\pi M_{\text{eff}}$ ,  $H_{A1}=2.45$  kOe, and  $H_{A2}=0.5$  kOe. Taking into account the lowest order contributions ( $4\pi M_{\text{eff}}$  and  $H_{A1}$ ), the out-of-plane hysteresis should reach saturation at a field of

$$4\pi M_{\text{eff}} + 2H_{A1} = 10.6 \text{ kOe} ,$$

which corresponds very well to the value obtained from a linear extrapolation of the magnetization slope at low fields. At higher fields, the well-known flattening of the magnetization curve due to higher-order contributions is observed.<sup>24</sup>

TABLE I. Properties of four uniaxial superlattices analyzed on the basis of Eqs. (2)–(5). All parameters were determined from fits to FMR data at various frequencies and orientations and are in very good agreement with the MOKE data as discussed in Sec. IV.

	$t_{\text{Co}}$ (Å)	$t_{\text{Cr}}$ (Å)	$N$	$4\pi M_{\text{eff}}$ (kOe)	$K_1/M$ (kOe)	$K_2/M$ (kOe)
SL1	35	37	10	5.7	2.45	0.5
SL2	23	25	20	1.5	2.8	0.65
SL3	17	20	30	−3.3	3.55	0.65
SL4	14	47	20	−7.2	3.59	0.55

The in-plane hard axis hysteresis [Fig. 1(b3)] exhibits, in principle, the same behavior. Considering, again, only lowest-order anisotropy, one should find saturation at fields of about  $2H_{A1}$  when extrapolated in the same manner. The analysis, however, can be complicated by small contributions of the second crystallographic domain which, in fact, has been detected with x-ray scattering in this sample. This may also be the reason for the nonzero remanence which is not expected for an *ideal* uniaxial system.<sup>25</sup>

Superlattice SL2 ( $t_{Co} = 23 \text{ \AA}$ ). Qualitatively, SL2 exhibits the same characteristics as SL1 but with an even stronger reduction of  $4\pi M_{eff}$ , which is of the order of only 1.5 kOe. The FMR and the MOKE data can be found in Fig. 2.

According to the x-ray data there should be a significant fraction of the second crystallographic domain in this sample. In fact, in the FMR spectra additional in-plane resonances have been observed with field positions roughly corresponding to those of the first crystallographic domain (and, consequently, comparable anisotropy parameters) but with an in-plane angle shifted by  $90^\circ$  (for clarity, we have plotted only the resonance fields of the more intense line). The in-plane anisotropy determined from the FMR data is even slightly larger than for SL1 which exhibited one strongly dominating *c* axis. On the other hand the in-plane hysteresis loops (which look

qualitatively similar to those of SL1) indicated a significantly reduced anisotropy with lower saturation field and higher remanence in the hard direction.

This behavior is exactly the one predicted in Sec. III B. The reduced anisotropy deduced from the MOKE data represents the overall anisotropy of the sample in which the anisotropies of the two domains partially cancel out each other whereas the FMR data refer to each region separately. In addition, one can try to get some information about the distribution of the two domains from the intensity ratio of the resonances in the FMR experiment and of the x-ray diffraction peaks. The latter yielded a ratio of the crystallographic domains slightly smaller than 3:1 whereas the ratio of the corresponding FMR signals was well above that (however, both values are difficult to evaluate precisely). This may be taken as an indication that some parts of the different domains are magnetically coupled to each other and other parts are not, resulting in the observed change of the FMR intensity ratio in comparison with the structural data, and, to some extent, also in a reduction of the effective anisotropy of each domain as compared to bulk values.

Superlattice SL3 ( $t_{Co} = 17 \text{ \AA}$ ). This is a typical example of a sample in the transition range of the anisotropy in which  $4\pi M_{eff}$  is already negative but the out-of-plane hysteresis loop shows essentially zero remanence (see Fig. 3). As in the case of SL1 and SL2, the saturation field

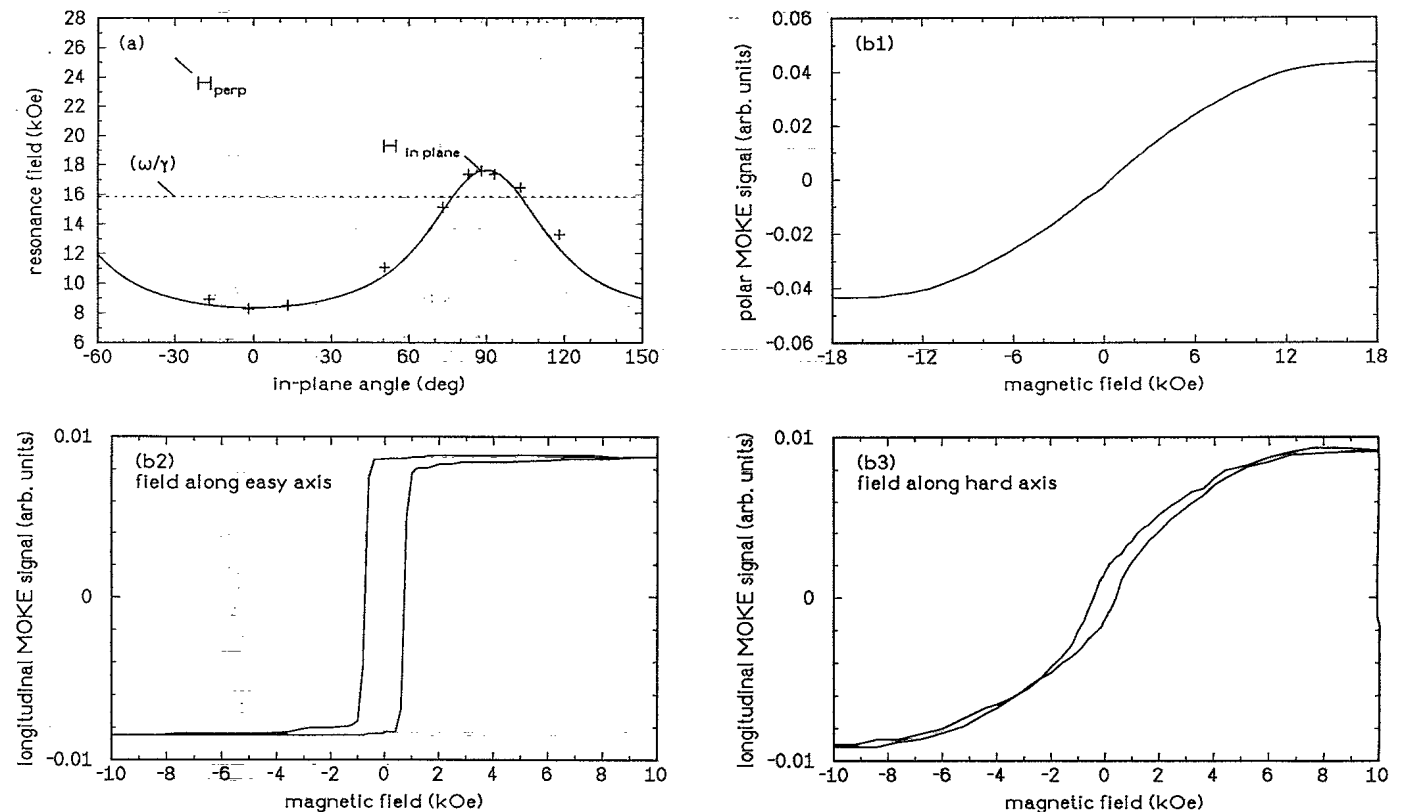


FIG. 1. (a) FMR line positions in-plane ( $H_{in-plane}$ ) and out-of-plane ( $H_{perp}$ ) at 48.80 GHz for superlattice SL1 ( $t_{Co} = 35 \text{ \AA}$ ). The solid line is a fit to the data using Eq. (4). For the purpose of comparison  $(\omega/\gamma)$  is shown which represents the resonance field of a perfectly isotropic ferromagnet. (b) Hysteresis loops measured by MOKE, (b1) polar (out-of-plane) configuration, (b2) longitudinal (in-plane) configuration with the field along the easy axis, and (b3) longitudinal configuration along the hard axis.

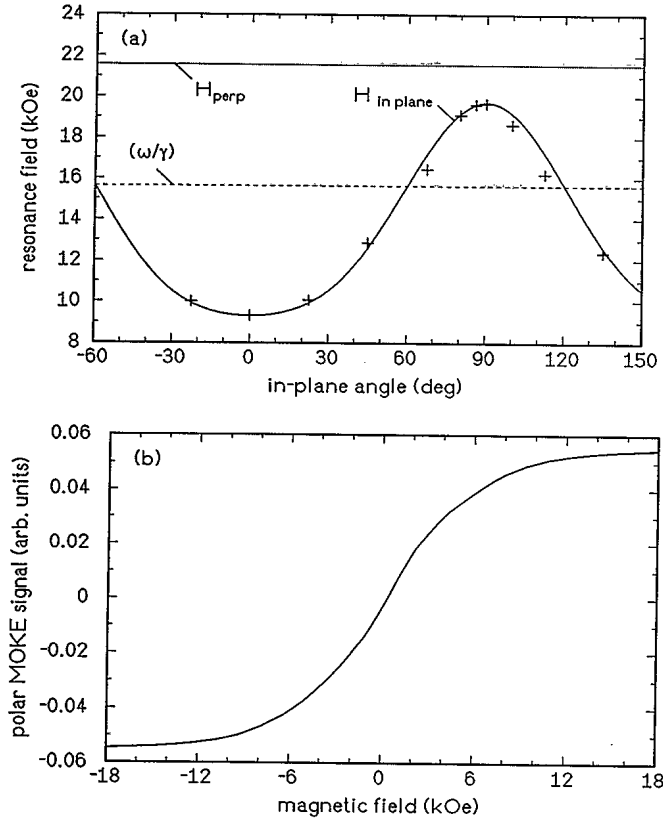


FIG. 2. (a) Same as Fig. 1(a) for superlattice SL2 ( $t_{\text{Co}} = 23 \text{ \AA}$ ). (b) Hysteresis loop measured by polar MOKE.

due to lowest-order contributions should be at about  $4\pi M_{\text{eff}} + 2H_{A1} = 3.7 \text{ kOe}$ , which is in excellent agreement with the extrapolation from the hysteresis loop. The in-plane FMR field in the hard direction is clearly above the perpendicular one, whereas the field position of the resonance in the easy direction in-plane is the lowest of all. The anisotropy energies of these principal axes are in the corresponding order

$$F(\parallel, \text{easy axis}) < F(\perp) < F(\parallel, \text{hard axis}),$$

which is a rather unusual situation.

Superlattice SL4 ( $t_{\text{Co}} = 14 \text{ \AA}$ ). The sample SL4 (see Fig. 4) with a Co thickness of  $14 \text{ \AA}$  represents the region of the switching of the magnetization. The resonance fields for the perpendicular orientation and for the in-plane easy axis are quite close (and both below  $\omega/\gamma$ ), whereas the line position for the in-plane hard axis is significantly above  $\omega/\gamma$ .

For  $t_{\text{Co}} \leq 14 \text{ \AA}$ , the samples tend to be magnetized along the film normal. This switching depends on the exact value of the in-plane anisotropy. The polar hysteresis becomes more square-type for smaller  $t_{\text{Co}}$  (see also the loops shown in Ref. 12).

## 2. In-plane fourfold samples

It is obvious that details of the in-plane anisotropy of the samples with dominatingly fourfold symmetry will depend on the growth conditions and the corresponding

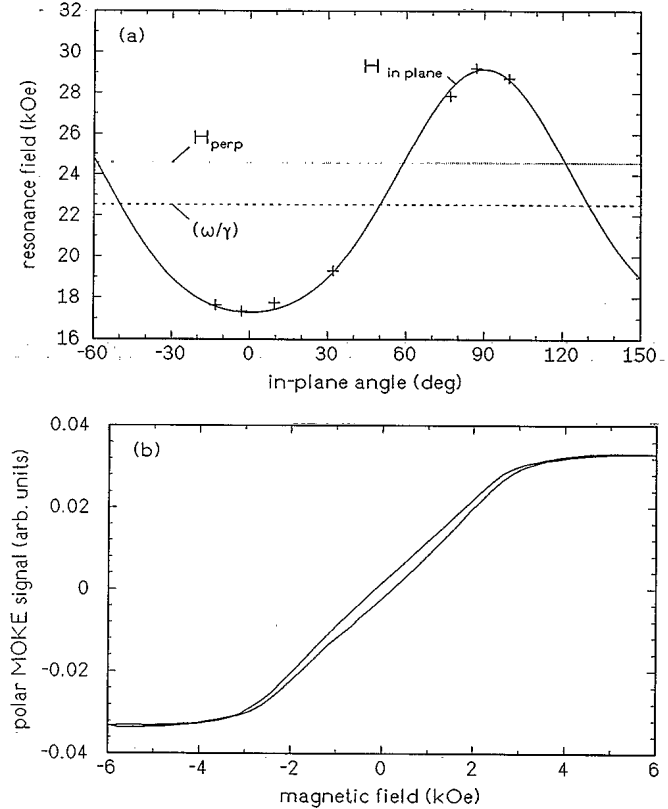


FIG. 3. (a) Same as Fig. 1(a) for superlattice SL3 ( $t_{\text{Co}} = 17 \text{ \AA}$ ). Here the measurements at  $69.68 \text{ GHz}$  are shown. The values of the resonance fields at  $48.80 \text{ GHz}$  for out-of-plane, in-plane easy, and in-plane hard axis are, respectively,  $17.8$ ,  $10.6$ , and  $22.6 \text{ kOe}$ . (b) Hysteresis loop measured by polar MOKE. Note that in spite of the already negative  $4\pi M_{\text{eff}}$  the remanence is almost zero. This is due to the strong in-plane anisotropy as described in the text.

coupling of the two domains. It appeared that samples with fourfold anisotropy could be found mainly for very low Co thicknesses.

A good example is the superlattice  $[\text{Co}_{12}\text{Cr}_{28}]_{10}$  for which also the analysis of the x-ray diffraction peak intensities yielded equivalent contributions from the two  $c$  axes. With  $t_{\text{Co}} = 12 \text{ \AA}$  the sample is expected to be perpendicularly magnetized which was confirmed by the polar hysteresis loop and the FMR line positions which are shown in Fig. 5. Unfortunately, the FMR signals became very weak when approaching the in-plane hard axes which now correspond to the two  $c$  axes.

The fit according to Eqs. (8) and (9) yields the parameters  $4\pi M_{\text{eff}}^* = -4.5 \text{ kOe}$ ,  $g = 2.19$ , and  $H_{A2} = 1.4 \text{ kOe}$ . The in-plane anisotropies found in other fourfold samples were of the same order as for this specimen. The value of  $4\pi M_{\text{eff}}^*$  is consistent with those obtained for the in-plane uniaxial samples. From Fig. 6 one can see that for a thickness of  $12 \text{ \AA}$  an out-of-plane anisotropy of about  $-10 \text{ kOe}$  (following the definition of  $4\pi M_{\text{eff}}^*$  for uniaxial samples) is to be expected. The difference  $-4.5 \text{ kOe} - (-10 \text{ kOe}) = 5.5 \text{ kOe}$  then corresponds to the term  $H_{A1} + 2H_{A2}$  in the definition of  $4\pi M_{\text{eff}}^*$  and is in good

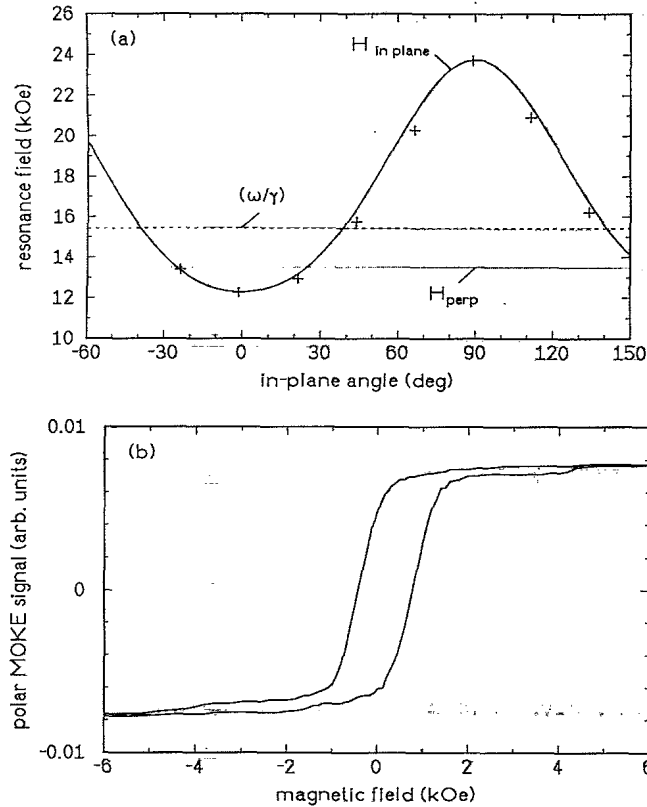


FIG. 4. (a) Same as Fig. 1(a) for superlattice SL4 ( $t_{\text{Co}} = 14 \text{ \AA}$ ). (b) Hysteresis loop measured by polar MOKE. This sample is in the transition region where the magnetization switches out-of-plane. From the analysis of the FMR data one finds that  $4\pi M_{\text{eff}}$  and  $2H_{A1}$  essentially cancel out each other. However, the hysteresis is still not square type; the remanent magnetization is about 70%.

agreement with bulk values of the magnetocrystalline anisotropy parameters.

Another superlattice with comparable structure except for a lower Cr thickness of  $12 \text{ \AA}$  yielded essentially the same anisotropy but exhibited almost zero remanence indicating an antiferromagnetic alignment of the layers. A

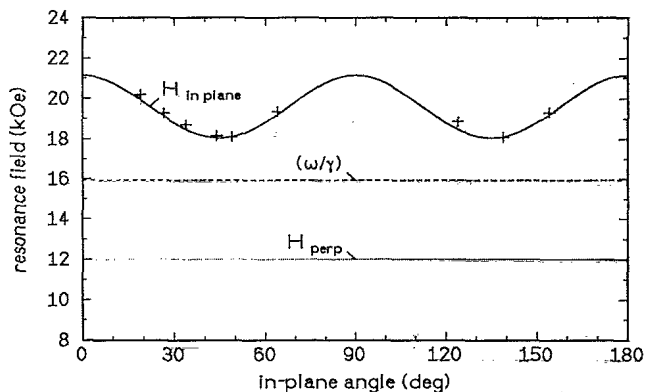


FIG. 5. FMR line positions in-plane and out-of-plane at  $48.80 \text{ GHz}$  for the superlattice  $[\text{Co}_{12}\text{Cr}_{28}]_{10}$  with fourfold anisotropy. The solid line is a fit to the data using Eq. (8).

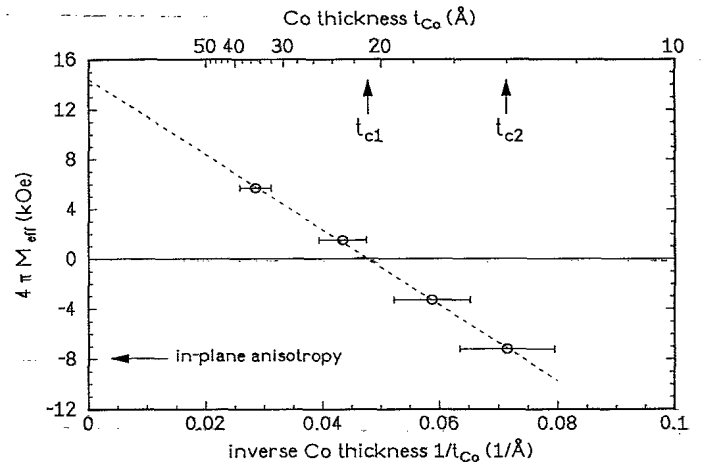


FIG. 6. Effective magnetization as a function of inverse Co thickness for in-plane uniaxial superlattices measured by both FMR and MOKE [ $4\pi M_{\text{eff}} = 4\pi M - 2(2K_s)/(Mt_{\text{Co}})$ ]. The broken line is a fit to the data. We have defined two critical thicknesses,  $t_{c1}$  and  $t_{c2}$ , representing, respectively, the change of sign of  $4\pi M_{\text{eff}}$  and the switching of the magnetization to the film normal as the easy axis. Due to the strong in-plane anisotropy,  $t_{c1}$  and  $t_{c2}$  differ significantly. For details see text.

detailed investigation of the coupling properties will be published in a forthcoming paper.

Our model of two coupled domains also describes very well two other systems exhibiting the same structure of Co. The first is Co grown directly on  $\text{MgO}(001)$ , prepared in our laboratory. The samples of that series show perfect fourfold symmetry of the in-plane FMR line position. The anisotropy parameter is smaller than that of the present  $\text{Co}/\text{Cr}(001)$  layers on sapphire which we think is at least partly due to a lower crystalline quality with broader in-plane rocking curves of Co on MgO (for details see Ref. 26). Secondly, in a recent publication epitaxially grown  $\text{Co}/\text{Cr}$  bilayer films on  $\text{MgO}(001)$  substrates were investigated.<sup>27</sup> The authors also observed two  $c$  axes and a resulting fourfold anisotropy. The orientation of the easy axes deduced from VSM hysteresis loops is in accord with our model but further analysis is difficult as no quantitative statements were made.

As it has already been pointed out in Sec. II we concentrate on superlattices as they can be structurally characterized in great detail by x rays. Besides them we have also grown a number of single layers of various thicknesses. The results from these films were in agreement with those obtained from the superlattices with respect to all parameters discussed here. However, the interpretation of the data was complicated as the in-plane anisotropy was often not one of the limiting cases, i.e., neither clearly uniaxial nor fourfold.

## B. Analysis

### 1. In-plane anisotropy

As can be seen from Table I, the in-plane anisotropy parameters,  $K_1/M$  and  $K_2/M$ , are essentially the same for all uniaxial samples and comparable to the bulk

values ( $K_1/M \approx 3.6$  kOe;  $K_2/M \approx 0.8$  kOe). Even for bulk data a relatively broad distribution of values is found in the literature.<sup>15,20,28,29</sup> Apparently, the *sum* of  $K_1$  and  $K_2$  scatters less than  $K_1$  and  $K_2$  each when comparing different works.

For our samples there only seems to be a weak tendency of a decreased  $H_{A1}$  at larger thicknesses. However, since already small differences of the contribution from the second crystallographic domain may have a pronounced impact on the effective values of  $H_{A1}$  and  $H_{A2}$ , it is hardly possible to extract unambiguously a systematic behavior.

Concerning the fourfold samples, our model has successfully predicted the orientation of the easy axes for the Co/Cr(001) samples of the present study as well as for the other two mentioned systems grown on MgO(001). As in these samples the in-plane anisotropy will depend sensitively on details of the microstructure and the associated coupling of the crystallographic domains, the *quantitative* result may not agree precisely with the model.

## 2. Out-of-plane anisotropy

In Fig. 6 we plot the out-of-plane anisotropy  $4\pi M_{\text{eff}}$  against the inverse thickness of the Co layers. We limit ourselves to only the in-plane uniaxial samples because for those the effective out-of-plane anisotropy can be separated from  $K_1$  and  $K_2$  terms which is more difficult for the case of in-plane fourfold symmetry.

The most striking feature of Fig. 6 concerns the critical thickness of the system Co/Cr(001). To be precise, we need to introduce *two* critical thicknesses,  $t_{c1}$  for the change of sign of  $4\pi M_{\text{eff}}$  and  $t_{c2}$  for the switching of the magnetization to the film normal as the easy axis. Due to the strong in-plane anisotropy  $t_{c1}$  and  $t_{c2}$  differ significantly.  $t_{c1}$  is about 21 Å whereas  $t_{c2}$  is approximately 14 Å (see discussion of SL4 above).

The fit in Fig. 6 yields  $4\pi M_{\text{eff}} = 14.5$  kOe for the intersection at  $1/t_{\text{Co}} = 0$  and  $K_s/M = 76$  kOe Å from the slope. The value of 14.5 kOe (one would expect  $\sim 18$  kOe as the bulk value) already indicates a reduced magnetic moment in our samples which, in fact, was confirmed by measurements with a Faraday balance. We found a magnetization  $M$  of the order of 1000 emu/cm<sup>3</sup> for most of the samples (1430 emu/cm<sup>3</sup> for bulk). Apparently, there was no strictly systematic thickness dependence, however, the tendency of a stronger reduced moment at lower  $t_{\text{Co}}$ . A reduction of the magnetic moment has also been found by other groups for Co/Cr superlattices prepared by different methods and in different orientations.<sup>30</sup> The mechanism for this is thought to be related to the fact that Co-Cr alloys become nonmagnetic already at about 25 at. % Cr.

If we use a value of  $M = 1000$  emu/cm<sup>3</sup>, we obtain a surface anisotropy  $K_s = 0.76$  erg/cm<sup>2</sup> which is remarkably high, in agreement with a large  $t_{c1}$ . One may expect  $K_s$  to be even higher for the region of larger thicknesses where the magnetization should reach the bulk value.

Due to the heavy distortion of the lattice in our samples, magnetoelastic interactions may be considered as a possible source for  $K_s$ . They, in fact, yield a considerable

contribution but it is not possible to explain the strong thickness dependence of the out-of-plane anisotropy only on the basis of this mechanism.<sup>12</sup>

We think that electronic effects at the interface are likely to play an important role. It is interesting to see that whereas for Co/ $X$  with  $X$  from the end of the Fe group (e.g., Ni or Cu)  $K_s$  remains well below our value for Co/Cr, the system Co/V was recently found to exhibit also a large  $K_s$  (1.05 erg/cm<sup>2</sup>).<sup>31</sup> The fact that both Cr and V are situated at the beginning of the Fe group may suggest a tendency for  $K_s$  in Co/ $X$  systems with higher values for those  $X$  having few 3d electrons but, of course, in view of the *structural* differences between these systems such a regularity based solely on the band filling may be hard to prove. As it is shown below, the  $g$  factor significantly increases for thin Co on Cr(001) which indicates that changes of the electronic properties occur.

We remark that the effective out-of-plane anisotropy field,  $H_A$ , as defined in Ref. 12, contained contributions from  $K_1$  and  $K_2$ , and, therefore, the  $1/t_{\text{Co}}$  plot in Ref. 12 appears to be shifted if compared with Fig. 6 of the present paper. As in that work we concentrated mainly on in-plane fourfold samples where  $K_1$  cannot be separated from the effective out-of-plane anisotropy [see Eqs. (7)–(10)], a direct comparison with the  $H_A$  values is difficult. The most important feature of the plot in that paper is, however, the critical thickness for the switching of the magnetization which corresponds exactly to  $t_{c2}$  defined above showing that the data are consistent.

## 3. $g$ factor

It was already mentioned that the  $g$  factor is related to the microscopic properties, namely the ratio of the spin moment,  $\mu_S$ , and the orbital moment,  $\mu_L$ . For an analysis of  $g$  in bulk 3d metals see, e.g., Ref. 32.

The  $g$  factor of some Co/Cr(001) samples is plotted in Fig. 7 versus  $1/t_{\text{Co}}$ . We have chosen the inverse thickness on the  $x$  axis as a generally typical scale in thin-film magnetism. This should not suggest that  $g$  has to follow a linear  $1/t_{\text{Co}}$  dependence. For low thicknesses,  $g$  and consequently the relative contribution of the orbital moment is found to increase. Using the relationship<sup>32</sup>

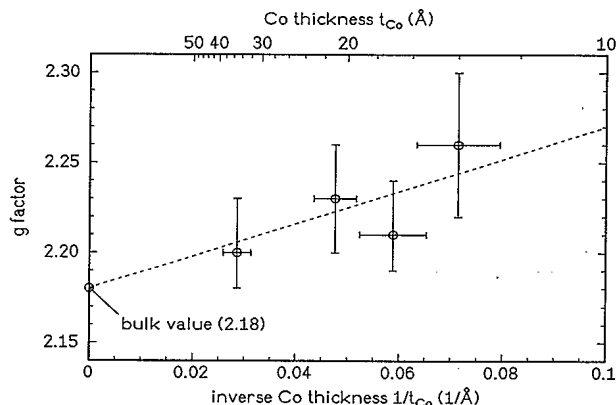


FIG. 7.  $g$  factor as a function of inverse Co thickness. The broken line is a guide to the eye. For a discussion see text.



$$\frac{\mu_L}{\mu_S} = \frac{g}{2} - 1 \quad (11)$$

the bulk value of  $g$  (2.18) corresponds to a ratio  $\mu_L/\mu_S$  of 0.09. For Co/Cr(001) with  $t_{\text{Co}} = 14 \text{ \AA}$ , we find a  $g$  factor of  $2.26 \pm 0.04$ . This means that the relative orbital contribution is then enhanced to about 13% of the spin contribution. This observation is in agreement with preliminary results from x-ray magnetic circular dichroism (MCD) measurements indicating also an increase of  $\mu_L/\mu_S$ .<sup>33</sup>

We note that despite the undoubtedly high power of MCD the determination of the  $g$  factor by FMR is of great use, most especially as there still seem to be open questions with respect to the interpretation of MCD spectra on the basis of sum rules.<sup>34</sup> Additionally, in the case of atoms having an environment without cubic symmetry non-negligible dipolar contributions may cause difficulties. Therefore, a comparison of both methods in the future should contribute to the understanding of MCD spectra and, hence, of magnetism on the microscopic level in general.

Changes in the orbital moment in thin layers were also the result of theoretical investigations, in both first-principles calculations,<sup>34,35</sup> and also those using a tight-binding approach.<sup>36</sup> It was shown that there is a close relationship between the magnetocrystalline (surface) anisotropy and the orbital moment as can be naively expected.<sup>37</sup> However, a direct comparison with these calculations is difficult and especially for our system, the theory may face considerable complications due to the significant distortion of the lattice and possible strong electronic interactions of Co and Cr.

## V. SUMMARY

FMR and MOKE studies were performed on Co/Cr(001) thin films and superlattices grown on  $\text{Al}_2\text{O}_3(1\bar{1}02)$  substrates by the MBE method. The structural characterization by RHEED and x-ray scattering in various geometries revealed that Co grows in the hcp phase with its  $c$  axis in-plane and with an anomalous

out-of-plane lattice expansion as a precursor of a structural phase transition from hcp to bcc.

It was found that there are two possible orientations for the  $c$  axis in the plane. The effects of these two structural domains are accounted for by a model for the magnetocrystalline anisotropy with either magnetically coupled or uncoupled crystallographic domains. Both cases are found in the experiment exploiting the fact that by FMR magnetically nonequivalent constituents of a sample can be identified by their respective resonances.

Due to the strong in-plane anisotropy of the  $c$  axis a rather unusual situation appears: the switching of the magnetization to the film normal occurs at a significantly lower critical thickness  $t_{c2} \approx 14 \text{ \AA}$  than the change of sign of  $4\pi M_{\text{eff}}$  at  $t_{c1} \approx 21 \text{ \AA}$ .

Good quantitative agreement between FMR and MOKE was found. The in-plane anisotropy parameters,  $K_1/M$  and  $K_2/M$ , exhibit no significant thickness dependence as determined from the uniaxially dominated samples. The surface anisotropy was found to be relatively large ( $K_s = 0.76 \text{ erg/cm}^2$ ) using a magnetic moment ( $1000 \text{ emu/cm}^3$ ) smaller than that of bulk Co. The  $g$  factor as a measure for the strength of the orbital moment relative to the spin contribution is found to increase for thin Co layers.

The results of the present study may also be helpful for the systematic investigation of the interlayer coupling which is often accompanied and complicated by anisotropy effects, particularly when the anisotropy is as strong as in Co/Cr(001).

## ACKNOWLEDGMENTS

The authors would like to thank Dr. J. J. Krebs and Dr. G. A. Prinz (Naval Research Washington) for valuable discussions and for providing FMR data of bcc Co. The help of J. Pflaum and Dr. Th. Orth (Ruhr-Universität Bochum) with some computer programs and with the proofreading of the manuscript is gratefully acknowledged. We also thank D. Schmitz (KFA Jülich) for providing unpublished MCD data. This work was supported by the Deutsche Forschungsgemeinschaft (SFB 166).

\*Present address: Neutron Scattering Lab., Dept. of Materials Science and Engineering, Japan Atomic Energy Research Institute, Tokai, Naka, Ibaraki 319-11, Japan.

<sup>†</sup>Present address: Institut für Materialwissenschaften, Bergische Universität und Gesamthochschule Wuppertal, 42285 Wuppertal, Germany.

<sup>1</sup>U. Gradmann, *J. Magn. Magn. Mater.* **100**, 481 (1991).

<sup>2</sup>B. Heinrich and J. F. Cochran, *Adv. Phys.* **42**, 523 (1993).

<sup>3</sup>G. A. Prinz, *J. Magn. Magn. Mater.* **100**, 469 (1991).

<sup>4</sup>G. A. Prinz, *Phys. Rev. Lett.* **54**, 1051 (1985).

<sup>5</sup>J. A. C. Bland, R. D. Bateson, P. C. Riedi, R. G. Graham, H. J. Lauter, J. Penfold, and C. Shakleton, *J. Appl. Phys.* **69**, 4989 (1991).

<sup>6</sup>V. L. Moruzzi, P. M. Marcus, K. Schwarz, and P. Mohn, *J. Magn. Magn. Mater.* **54-57**, 955 (1986).

<sup>7</sup>See, e.g., J. J. de Miguel, A. Cebollada, J. M. Gallego, R.

Miranda, C. M. Schneider, P. Schuster, and J. Kirschner, *J. Magn. Magn. Mater.* **93**, 1 (1991); P. Bödeker, A. Abromeit, K. Bröhl, P. Sonntag, N. Metoki, and H. Zabel, *Phys. Rev. B* **47**, 2353 (1993); D. Weller, G. R. Harp, R. F. C. Farrow, A. Cabollada, and J. Sticht, *Phys. Rev. Lett.* **72**, 2097 (1994).

<sup>8</sup>B. Heinrich, J. F. Cochran, M. Kowalewski, J. Kirschner, Z. Celinski, A. S. Arrott, and K. Myrtle, *Phys. Rev. B* **44**, 9348 (1991).

<sup>9</sup>For the magnetic properties of bcc Co, see also, G. A. Prinz, C. Vittora, J. J. Krebs, and K. B. Hathaway, *J. Appl. Phys.* **57**, 3672 (1985); J. M. Karanikas, R. Sooryakumar, G. A. Prinz, and B. T. Jonker, *J. Appl. Phys.* **69**, 6120 (1991), and references therein.

<sup>10</sup>W. Donner, N. Metoki, A. Abromeit, and H. Zabel, *Phys. Rev. B* **48**, 14 745 (1993).

<sup>11</sup>N. Metoki, W. Donner, and H. Zabel, *Phys. Rev. B* **49**, 17 351

- (1994).
- <sup>12</sup>W. Donner, N. Metoki, F. Schreiber, Th. Zeidler, and H. Zabel, *J. Appl. Phys.* **75**, 6421 (1994).
- <sup>13</sup>P. V. Mitchell, A. Layadi, N. S. VanderVen, and J. O. Artman, *J. Appl. Phys.* **57**, 3976 (1985); J. O. Artman, *J. Appl. Phys.* **61**, 3137 (1987), and references therein.
- <sup>14</sup>N. Metoki *et al.* (unpublished).
- <sup>15</sup>D. M. Paige, B. Szpunar, and B. K. Tanner, *J. Magn. Magn. Mater.* **44**, 239 (1984).
- <sup>16</sup>F. Schreiber, A. Soliman, P. Bödeker, R. Meckenstock, K. Bröhl, J. Pelzl, and I. A. Garifullin, *J. Appl. Phys.* **75**, 6492 (1994); F. Schreiber, A. Soliman, P. Bödeker, R. Meckenstock, K. Bröhl, and J. Pelzl, *J. Magn. Magn. Mater.* **135**, 215 (1994).
- <sup>17</sup>The form of the resonance condition for the case of one single domain is equivalent to the one given in Ref. 20 except for an exchange of the two brackets on the right-hand side of Eq. (4) in Ref. 20 and a misprint in that equation in Ref. 20 [term  $4\pi M$  missing in the second line of Eq. (4)].
- <sup>18</sup>J. Smit and H. G. Beljers, *Philips Res. Rep.* **10**, 113 (1955); S. V. Vonsovskii, *Ferromagnetic Resonance* (Pergamon, New York, 1966).
- <sup>19</sup>For a recent description of FMR and its applications to thin films see, e.g., B. Heinrich, in *Ultrathin Magnetic Structures*, edited by B. Heinrich and J. A. C. Bland (Springer, Berlin, 1994), Vol. II.
- <sup>20</sup>Z. Frait, *Brit. J. Appl. Phys.* **15**, 993 (1964).
- <sup>21</sup>J. J. Krebs (private communication).
- <sup>22</sup>B. Heinrich, K. B. Urquhart, A. S. Arrott, J. F. Cochran, K. Myrtle, and S. T. Purcell, *Phys. Rev. Lett.* **59**, 1756 (1987).
- <sup>23</sup>S. T. Purcell, H. W. van Kasteren, E. C. Cosman, W. B. Zeper, and W. Hoving, *J. Appl. Phys.* **69**, 5640 (1991).
- <sup>24</sup>W. Sucksmith and J. E. Thompson, *Proc. R. Soc. London Ser. A* **255**, 362 (1954).
- <sup>25</sup>E. C. Stoner and E. P. Wohlfarth, *Proc. R. Soc. London Ser. A* **240**, 599 (1948).
- <sup>26</sup>Yu. V. Goryunov, M. G. Khusainov, I. A. Garifullin, F. Schreiber, J. Pelzl, Th. Zeidler, K. Bröhl, N. Metoki, and H. Zabel, *J. Magn. Magn. Mater.* (to be published).
- <sup>27</sup>A. Nakamura and M. Futamoto, *Jpn. J. Appl. Phys.* **32**, L1410 (1993).
- <sup>28</sup>F. Ono, *J. Phys. Soc. Jpn.* **50**, 2564 (1981).
- <sup>29</sup>M. B. Stearns, in *Numerical Data and Functional Relationships in Science and Technology*, edited by K.-H. Hellwege and O. Madelung, Landolt-Börnstein, New Series, Group III, Vol. 19a (Springer, Berlin, 1986).
- <sup>30</sup>Y. Henry, C. Mény, A. Dinia, and P. Panissod, *Phys. Rev. B* **47**, 15 037 (1993); P. Boher, F. Giron, Ph. Houdy, P. Beauvilain, C. Chappert, and P. Veillet, *J. Appl. Phys.* **70**, 5507 (1991); M. B. Stearns, C. H. Lee, and T. L. Groy, *Phys. Rev. B* **40**, 8256 (1989).
- <sup>31</sup>P. J. H. Bloemen, Ph.D. thesis, Eindhoven, 1993; H. A. M. de Gronckel, Ph.D. thesis, Eindhoven, 1993.
- <sup>32</sup>A. J. P. Meyer and G. Aşch, *J. Appl. Phys.* **32**, 330S (1961); R. A. Reck and D. L. Fry, *Phys. Rev.* **184**, 492 (1969).
- <sup>33</sup>D. Schmitz *et al.* (unpublished).
- <sup>34</sup>R. Wu, D. Wang, and A. J. Freeman, *J. Magn. Magn. Mater.* **132**, 103 (1994), and references therein.
- <sup>35</sup>A. J. Freeman and R. Wu, *J. Magn. Magn. Mater.* **100**, 497 (1991), and references therein.
- <sup>36</sup>P. Bruno, *Phys. Rev. B* **39**, 865 (1989); P. Bruno and J.-P. Renard, *Appl. Phys. A* **49**, 499 (1989).
- <sup>37</sup>See, also, recent experimental investigations, e.g., D. Weller, Y. Wu, J. Stöhr, M. G. Samant, B. D. Hermsmeier, and C. Chappert, *Phys. Rev. B* **49**, 12 888 (1994); and references therein.